Oscillations of flexible orthotropic meshed micropolar Timoshenko's plate

J Awrejcewicz, E.Yu. Krylova, I.V. Papkova, V.A. Krysko

*Abstract:*The oscillation's theory of a geometrically nonlinear micropolar orthotropic meshed plate under the action of a normal distributed load is constructed in this paper. The plate's material as a Cosserat continuum with constrained particle rotation (pseudocontinuum). As a result, an additional independent parameter of length l associated with the symmetric bending-torsion tensor will appear in the model. The panel consists of n sets of identical edges, what allows to apply the continuous G. I. Pshenichnov's model. The equilibrium equations for the plate element and the boundary conditions are obtained from the Ostrogradskyi-Gamilton variation principle on the basis of S.P.Timoshenko's kinematic hypotheses. Geometric nonlinearity is taken into account according to the Theodore von Karman model. The system of differential equations in partial derivatives is reduced to theODE system using the Bubnov-Galerkin method. Using the establishment method,theinfluence of the normal load, an additional length's parameter l, and mesh's geometry on the orthotropic plate's behavior consisting of two families of mutually orthogonal edges has been studied.

1. Formulation of the problem

In this paper the mathematical model of the geometrically nonlinear microdimensional anisotropic cylindrical mesh panel oscillations based on the Tymoshenko's hypotheses is constructed. The panel consists n families of densely spaced edges of the same material, which makes it possible to use the G. I. Pshenichnov continuum model [1]. Thus, the original mesh panel is replaced by a continuous layer. In the general formulation, it is necessary to consider the anisotropic material of the panel. Consider a panel assigned to the orthogonal coordinate system, consisting of two families of rods located at angles $\varphi_1 = -\varphi_2$ to the Ox axis.This mesh geometry allows us to consider the panel material as orthotropic, in which the directions of orthotropy coincide with the directions ofcoordinate lines.For a structurally orthotropic panel, we can write the relationship between Young's modulus (E_1 , E_2)and Poisson's ratio (ν_{21} , ν_{12})through the reduced Young's modulus and Poisson's ratio for the isotropic case (E , ν)[2]:

$$E_1 = \frac{E}{m_1},\ E_2 = m_2 E,\ \nu_{21} = \nu,\ \nu_{12} = \frac{\nu}{m_1 m_2},\ G_{13} = n_1 G_{12},\ G_{23} = n_2 G_{12},$$

where m_1, m_2, n_1, n_2 are constants depending on the panel material.Due to mathematical and computational difficulties, many authors [3,4] apply an additional restriction on the shell material when they study orthotropic shells. The shear modulus is not an independent parameter, but is expressed through Young's module and Poisson's ratio, as in the case of isotropy: $G_{12} = \dfrac{E}{2(1+\nu)}$.

Micro size plates and shells are actively used as elements of NEMS and MEMS. Thus, the development of reliable mathematical models is necessary to study the modes of their operation in statics and dynamics. The application of classical mechanics methods in this case will lead to a high error of the result since they do not take into account scale effects.To take into account scale effects at the micro and nano level, many papers use micropolar (moment, asymmetric theory) [5-12]. For continuous shells, a theory was constructed in [13] that takes into account the orthotropy of the material. In this paper, we also use a modified moment theory. That is, along with the usual stress field, moment stresses are also considered.It is assumed that the fields of displacements and rotations are not independent.Given [14] and assuming $n_1 = m_1$ and $n_2 = m_2$ we write the defining relations:

$$\sigma_{xx} = \frac{m_2 E}{m_1 m_2 - \nu^2}\left[e_{xx} + \nu e_{yy}\right],\ \sigma_{yy} = \frac{m_2 E}{m_1 m_2 - \nu^2}\left[m_1 m_2 e_{yy} + \nu e_{yy}\right],$$

$$\sigma_{xy} = \frac{E}{2(1+\nu)} e_{xy},\ \sigma_{xz} = \frac{m_1 E}{2(1+\nu)} e_{zx},$$

$$\sigma_{yz} = \frac{m_2 E}{2(1+\nu)} e_{yz},\ m_{mk} = \frac{El^2}{1+\nu}\chi_{mk}.$$

The non-zero components of the strain tensor can be written in the form:

$$e_{xx} = \frac{\partial u}{\partial x} + \frac{1}{2}\left(\frac{\partial w}{\partial x}\right)^2 + z\frac{\partial \gamma_x}{\partial x},$$

$$e_{yy} = \frac{\partial v}{\partial y} + \frac{1}{2}\left(\frac{\partial w}{\partial y}\right)^2 - k_y w + z\frac{\partial \gamma_y}{\partial y},$$

$$e_{xy} = \frac{1}{2}\left(\frac{\partial u}{\partial y} + \frac{\partial v}{\partial x}\right) + \frac{\partial w}{\partial x}\frac{\partial w}{\partial y} + z\frac{1}{2}\left(\frac{\partial \gamma_x}{\partial y} + \frac{\partial \gamma_y}{\partial x}\right),$$

$$e_{yz} = \frac{1}{2}\left(\gamma_y + \frac{\partial w}{\partial y}\right),\ e_{xz} = \frac{1}{2}\left(\gamma_x + \frac{\partial w}{\partial x}\right),\ e_{zz} = 0.$$

The components of the symmetric bending-torsion tensor will take the form:

$$\chi_{xx} = \frac{1}{2}\left(-\frac{\partial \gamma_y}{\partial x} + \frac{\partial^2 w}{\partial x \partial y}\right),\ \chi_{yy} = \frac{1}{2}\left(\frac{\partial \gamma_x}{\partial y} - \frac{\partial^2 w}{\partial x \partial y}\right),$$

$$\chi_{zz}=\frac{1}{2}\left(-\frac{\partial\gamma_y}{\partial x}+\frac{\partial\gamma_x}{\partial y}\right),\ \chi_{xy}=\frac{1}{4}\left(-\frac{\partial\gamma_y}{\partial y}+\frac{\partial\gamma_x}{\partial x}+\frac{\partial^2 w}{\partial y^2}-\frac{\partial^2 w}{\partial x^2}\right),$$

$$\chi_{xz}=\frac{1}{4}\left(\frac{\partial^2 v}{\partial x^2}-\frac{\partial^2 u}{\partial x\partial y}\right)+\frac{z}{4}\left(\frac{\partial^2\gamma_y}{\partial x^2}-\frac{\partial^2\gamma_x}{\partial x\partial y}\right),$$

$$\chi_{yz}=\frac{1}{4}\left(\frac{\partial^2 v}{\partial x\partial y}-\frac{\partial^2 u}{\partial y^2}\right)+\frac{z}{4}\left(\frac{\partial^2\gamma_y}{\partial x\partial y}-\frac{\partial^2\gamma_x}{\partial y^2}\right).$$

Here u,v,w - are the axial displacements of the plate middle surface in the directions x,y,z, respectively. γ_x and γ_y are the panel cross-section angles, k_y - is geometric parameter of panel's curvature, σ_{ij} - are components of the stress tensor, m_{ij} -are components of the tensor of higher order, l is additional independent material length parameter associated with the symmetric bending-torsion tensor. The equations of motion, boundary and initial conditions for an equivalent smooth panel were obtained from the variational principle of Ostrogradskiy-Hamilton. Then the forces and moments acting in the smooth panel were expressed in terms of the forces and moments acting in the original mesh panel [15].

As a result, the equations of motion of the micropolar mesh cylindrical panel elementtook the form:

$$A_{40}\frac{\partial}{\partial x}\left(N_{xx}\frac{\partial w}{\partial x}\right)+A_{22}\frac{\partial}{\partial x}\left(N_{yy}\frac{\partial w}{\partial x}\right)+A_{31}\frac{\partial}{\partial x}\left(T\frac{\partial w}{\partial x}\right)+2A_{31}\frac{\partial}{\partial x}\left(N_{xx}\frac{\partial w}{\partial y}\right)+2A_{13}\frac{\partial}{\partial x}\left(N_{yy}\frac{\partial w}{\partial y}\right)+$$
$$+2A_{22}\frac{\partial}{\partial x}\left(T\frac{\partial w}{\partial y}\right)+2A_{31}\frac{\partial}{\partial y}\left(N_{xx}\frac{\partial w}{\partial x}\right)+2A_{13}\frac{\partial}{\partial y}\left(N_{yy}\frac{\partial w}{\partial x}\right)+2A_{22}\frac{\partial}{\partial y}\left(T\frac{\partial w}{\partial x}\right)+A_{22}\frac{\partial}{\partial y}\left(N_{xx}\frac{\partial w}{\partial y}\right)+$$
$$+A_{04}\frac{\partial}{\partial y}\left(N_{yy}\frac{\partial w}{\partial y}\right)+A_{13}\frac{\partial}{\partial y}\left(T\frac{\partial w}{\partial y}\right)+A_{20}\frac{\partial Q_{zx}}{\partial x}+A_{11}\frac{\partial Q_{zy}}{\partial x}+A_{11}\frac{\partial Q_{zx}}{\partial y}+A_{02}\frac{\partial Q_{zy}}{\partial y}-$$
$$-k_y\left(A_{22}N_{xx}+A_{04}N_{yy}+A_{13}T\right)-\frac{1}{2}\left[\left(A_{40}-A_{22}\right)\frac{\partial^2 Y_{xx}}{\partial x\partial y}+\left(A_{22}-A_{04}\right)\frac{\partial^2 Y_{yy}}{\partial x\partial y}+\left(A_{31}-A_{13}\right)\frac{\partial^2 Y_{xy}}{\partial x\partial y}\right]-$$
$$-\frac{1}{2}\left[A_{31}\frac{\partial^2 Y_{xx}}{\partial y^2}+A_{13}\frac{\partial^2 Y_{yy}}{\partial y^2}+A_{22}\frac{\partial^2 Y_{xy}}{\partial y^2}+-A_{31}\frac{\partial^2 Y_{xx}}{\partial x^2}-A_{13}\frac{\partial^2 Y_{yy}}{\partial x^2}-A_{22}\frac{\partial^2 Y_{xy}}{\partial x^2}\right]=\rho h\frac{\partial^2 w}{\partial t^2}-\varepsilon\rho h\frac{\partial\ w}{\partial t}.$$

$$A_{40}\frac{\partial N_{xx}}{\partial x}+A_{22}\frac{\partial N_{yy}}{\partial x}+A_{31}\frac{\partial T}{\partial x}+A_{31}\frac{\partial N_{xx}}{\partial y}+A_{13}\frac{\partial N_{yy}}{\partial y}+A_{22}\frac{\partial T}{\partial y}$$
$$+\frac{1}{2}\left(A_{11}\frac{\partial^2 Y_{xz}}{\partial y^2}+A_{02}\frac{\partial^2 Y_{yz}}{\partial y^2}+A_{01}\frac{\partial^2 Y_{zz}}{\partial y^2}+A_{20}\frac{\partial^2 Y_{\alpha z}}{\partial x\partial y}+A_{11}\frac{\partial^2 Y_{\beta z}}{\partial x\partial y}+A_{10}\frac{\partial^2 Y_{zz}}{\partial x\partial y}\right)=\rho h\frac{\partial^2 u}{\partial t^2}-\varepsilon\rho h\frac{\partial\ u}{\partial t},$$

$$A_{22}\frac{\partial N_{xx}}{\partial y}+A_{04}\frac{\partial N_{yy}}{\partial y}+A_{13}\frac{\partial T}{\partial y}+A_{31}\frac{\partial N_{xx}}{\partial x}+A_{13}\frac{\partial N_{yy}}{\partial x}+A_{22}\frac{\partial T}{\partial x}$$
$$-\frac{1}{2}\left(A_{20}\frac{\partial^2 Y_{xz}}{\partial x^2}+A_{11}\frac{\partial^2 Y_{yz}}{\partial x^2}+A_{10}\frac{\partial^2 Y_{zz}}{\partial x^2}+A_{11}\frac{\partial^2 Y_{xz}}{\partial x\partial y}+A_{02}\frac{\partial^2 Y_{yz}}{\partial x\partial y}+A_{01}\frac{\partial^2 Y_{zz}}{\partial x\partial y}\right)=\rho h\frac{\partial^2 v}{\partial t^2}-\varepsilon\rho h\frac{\partial\ v}{\partial t},$$

$$A_{40}\frac{\partial M_{xx}}{\partial x}+A_{22}\frac{\partial M_{yy}}{\partial x}+A_{31}\frac{\partial H}{\partial x}+A_{31}\frac{\partial M_{xx}}{\partial y}+A_{13}\frac{\partial M_{yy}}{\partial y}+A_{22}\frac{\partial H}{\partial y}-A_{20}Q_{zx}-A_{11}Q_{zy}$$

$$+\frac{1}{2}\left(A_{22}\frac{\partial Y_{xx}}{\partial y}+A_{04}\frac{\partial Y_{yy}}{\partial y}+A_{13}\frac{\partial Y_{xy}}{\partial y}-A_{10}\frac{\partial Y_{xz}}{\partial y}-A_{01}\frac{\partial Y_{yz}}{\partial y}-A_{00}\frac{\partial Y_{zz}}{\partial y}+A_{31}\frac{\partial Y_{xx}}{\partial x}+A_{13}\frac{\partial Y_{yy}}{\partial x}+A_{22}\frac{\partial Y_{xy}}{\partial x}\right)$$

$$+\frac{1}{2}\left(A_{20}\frac{\partial^2 J_{xz}}{\partial x\partial y}+A_{11}\frac{\partial^2 J_{yz}}{\partial x\partial y}+A_{10}\frac{\partial^2 J_{zz}}{\partial x\partial y}+A_{11}\frac{\partial^2 J_{xz}}{\partial y^2}+A_{02}\frac{\partial^2 J_{yz}}{\partial y^2}+A_{01}\frac{\partial^2 J_{zz}}{\partial y^2}\right)=\rho h\frac{\partial^2\gamma_x}{\partial t^2}-\varepsilon\rho h\frac{\partial\gamma_x}{\partial t},$$

$$A_{22}\frac{\partial M_{xx}}{\partial y}+A_{04}\frac{\partial M_{yy}}{\partial y}+A_{13}\frac{\partial H}{\partial y}+A_{31}\frac{\partial M_{xx}}{\partial x}+A_{13}\frac{\partial M_{yy}}{\partial x}+A_{22}\frac{\partial H}{\partial x}-A_{11}Q_{zx}-A_{02}Q_{zy}-$$

$$-\frac{1}{2}\left(A_{40}\frac{\partial Y_{xx}}{\partial x}+A_{22}\frac{\partial Y_{yy}}{\partial x}+A_{31}\frac{\partial Y_{xy}}{\partial x}-A_{10}\frac{\partial Y_{xz}}{\partial x}-A_{01}\frac{\partial Y_{yz}}{\partial x}-A_{00}\frac{\partial Y_{zz}}{\partial x}_{zz}+A_{31}\frac{\partial Y_{xx}}{\partial y}+A_{13}\frac{\partial Y_{yy}}{\partial y}+A_{22}\frac{\partial Y_{xy}}{\partial y}\right)-$$

$$-\frac{1}{2}\left(A_{20}\frac{\partial^2 J_{xz}}{\partial x^2}+A_{11}\frac{\partial^2 J_{yz}}{\partial x^2}+A_{10}\frac{\partial^2 J_{zz}}{\partial x^2}+A_{11}\frac{\partial^2 J_{xz}}{\partial x\partial y}+A_{02}\frac{\partial^2 J_{yz}}{\partial x\partial y}+A_{01}\frac{\partial^2 J_{zz}}{\partial x\partial y}\right)=\rho h\frac{\partial^2\gamma_y}{\partial t^2}-\varepsilon\rho h\frac{\partial\gamma_y}{\partial t},$$

Where $A_{sk}=\sum_{j=1}^{n}\frac{\delta_j\,\mathrm{Cos}^s\varphi_j\,\mathrm{Sin}^k\varphi_j}{a_j};\ s,k=\overline{0,4}$, $\left(N_{xx},N_{yy},T\right)=\int_{-\frac{h}{2}}^{\frac{h}{2}}\left(\sigma_{xx},\sigma_{yy},\sigma_{xy}\right)dz,$

$\left(M_{xx},M_{yy},H\right)=\int_{-\frac{h}{2}}^{\frac{h}{2}}\left(\sigma_{xx},\sigma_{yy},\sigma_{xy}\right)zdz,\quad \left(Q_{xz},Q_{yz}\right)=\int_{-\frac{h}{2}}^{\frac{h}{2}}\left(\sigma_{xz},\sigma_{yz}\right)k_s dz,\quad Y_{xx}=\int_{-\frac{h}{2}}^{\frac{h}{2}}m_{xx}dz,\quad Y_{xy}=\int_{-\frac{h}{2}}^{\frac{h}{2}}m_{xy}dz,$

$Y_{\alpha z}=\int_{-\frac{h}{2}}^{\frac{h}{2}}m_{xz}dz,\quad x\rightleftarrows y,\quad Y_{zz}=\int_{-\frac{h}{2}}^{\frac{h}{2}}m_{zz}dz,\quad J_{xz}=\int_{-\frac{h}{2}}^{\frac{h}{2}}m_{xz}zdz,\quad x\rightleftarrows y,$ a_j - is the distance between edges of j-th set, δ_j – is the edge thickness of the j-th set, φ_j – is the angle between the x-axis and the edge axis of the j-th set, stresses with index j refer to rods, ρ - is the density of plate material, h - is the thickness of the panel, k_s - is the function that characterizes the lawdistributionof shear stresses across the panel thickness.

In this model, the bending stiffness of the rods in the plane tangent to the median surface of the panel is not taken into account, therefore, the orders of the differential equations systemsdescribing the behavior of mesh and solid panels coincide. The formulations of the boundary conditions of the corresponding boundary value problemsare coincide[1].

2. Numerical results

The purpose of this work is to study the effect of the materialmicro polarity and mesh geometry on the behavior of arectangular in plan cylindrical panel. The boundary conditions are therigidly clamped along the ends. The cylindrical panel is under the action of a normal distributed load $q(x,y)=const$.

The equations of motion, boundary and initial conditions are reduced to dimensionless form using the following parameters: $x = 2c\bar{x},\ y = 2b\bar{y},\ w = h\bar{w},\ \gamma_x = \frac{h}{2c}\bar{\gamma}_x,\ \gamma_y = \frac{h}{2b}\bar{\gamma}_y,\ u = \frac{h^2}{2c}\bar{u},$

$v = \frac{h^2}{2b}\bar{v},\ \delta = h\bar{\delta},\ a = h\bar{a},\ l = h\bar{l},\ k_y = \frac{1}{2b}\bar{k}_y,\ t = \frac{2c2b}{h}\sqrt{\frac{\rho}{E}}\bar{t},\ \varepsilon = \frac{h}{(2c)(2b)}\sqrt{\frac{E}{\rho}}\bar{\varepsilon},\ q = \frac{Eh^4}{(2c)^2(2b)^2}\bar{q}$,

where c, b - are plate's linear dimensions in x and y direction, ρ - is the panels material density, ε - dissipation coefficient.

Boundary conditions:

$$w = 0, \quad \frac{\partial w}{\partial x} = 0, \quad \frac{\partial w}{\partial y} = 0, \quad at \quad x = -1, \quad x = 1, \quad y = -1, \quad y = 1,$$

$$u = 0, \quad \frac{\partial u}{\partial x} = 0, \quad \frac{\partial u}{\partial y} = 0, \quad at \quad x = -1, \quad x = 1, \quad y = -1, \quad y = 1,$$

$$v = 0, \quad \frac{\partial v}{\partial x} = 0, \quad \frac{\partial v}{\partial y} = 0 \quad at \quad x = -1, \quad x = 1, \quad y = -1, \quad y = 1,$$

$$\gamma_x = 0, \quad \frac{\partial \gamma_x}{\partial x} = 0, \quad \frac{\partial \gamma_x}{\partial y} = 0 \quad at \quad x = -1, \quad x = 1, \quad y = -1, \quad y = 1,$$

$$\gamma_y = 0, \quad \frac{\partial \gamma_y}{\partial x} = 0, \quad \frac{\partial \gamma_y}{\partial y} = 0 \quad at \quad x = -1, \quad x = 1, \quad y = -1, \quad y = 1.$$

Initial conditions are equal zero.

We will consider a panel formed by two systems of identical mutually perpendicular edges $\varphi_1 = 45^\circ$ and $\varphi_2 = 135^\circ$, $a_1 = a_2 = a$, $\delta_1 = \delta_2 = \delta$. (Figure1)

The behavior of the system will be investigated using the establishment method. The dissipation coefficient is $\varepsilon_{cr} = 1$. The system of differential equations in partial derivatives is reduced to the ODE system using the Bubnov-Galerkin method. To satisfy the boundary conditions, we choose the functions $u,\ v,\ w,\ \gamma_x,\ \gamma_y$ in the following form:

$$u(x,y,t) = \sum_{ij} U(t)\mathrm{Sin}^2\left(\frac{2i\pi x}{c}\right)\mathrm{Sin}^2\left(\frac{j\pi y}{b}\right),$$

$$v(x,y,t) = \sum_{ij} V(t)\mathrm{Cos}^2\left(\frac{(2i-1)\pi x}{2c}\right)\mathrm{Cos}^2\left(\frac{(2j-1)\pi y}{2b}\right),$$

$$w(x,y,t) = \sum_{ij} W(t)\mathrm{Sin}^2\left(\frac{i\pi x}{c}\right)\mathrm{Sin}^2\left(\frac{j\pi y}{b}\right),$$

$$\gamma_x(x,y,t) = \sum_{ij} \Gamma_x(t)\mathrm{Sin}^2\left(\frac{i\pi x}{c}\right)\mathrm{Sin}^2\left(\frac{2j\pi y}{b}\right),$$

$$\gamma_y(x,y,t) = \sum_{ij} \Gamma_y(t)\mathrm{Sin}^2\left(\frac{2i\pi x}{c}\right)\mathrm{Sin}^2\left(\frac{2j\pi y}{b}\right).$$

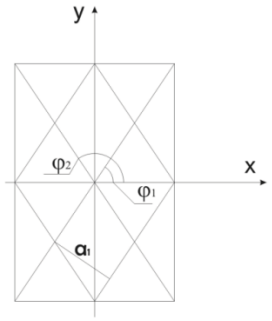

Figure 1. Plate grid geometry.

The Cauchy problem is solved by the Runge – Kutta method of the 4th order of accuracy.Experiment Parameters: $\nu = 0.3$, $\delta = h = 0.002$.

Table 1 shows the "deflection - load" dependences obtained by the Galerkin method and the finite difference method for a Timoshenko cylindrical micropolar mesh panel in the case of an isotropic material$\left(E = 1\,\text{TPa} \right)$. The results obtained by various methods are in good agreement.From the data of the table it is seen that the consideration of moment stresses leads to an increase in the bending stiffness of the panel.

Table 1

"Deflection - load" dependences obtained by the Galerkin method and the finite difference method

	$l = 0$		$l = 0.5$	
q	FDM	Galerkin	FDM	Galerkin
50	1.00688	0.93281	0.85688	0.90181
100	1.23579	1.20664	1.09991	1.18192
150	1.34555	1.39576	1.27119	1.37414
200	1.46420	1.54522	1.41382	1.52557
250	1.56740	1.67087	1.51180	1.65262
300	1.63434	1.78036	1.63388	1.76319
350	1.78429	1.87805	1.77992	1.86174
400	1.99430	1.96668	1.93685	1.95107
450	2.02916	2.04808	2.01818	2.03307
500	2.19714	2.12357	2.14709	2.10907
550	2.26987	2.19411	2.26537	2.18007

In the Figure 2 shows the dependences of the "deflection-load" for otrotropic and isotropic cases ($E_1 = 839.4\,\text{GPa}$ $E_2 = 964$ GPa. $E = 1000\,\text{GPa}$. $\nu = 0.3$)

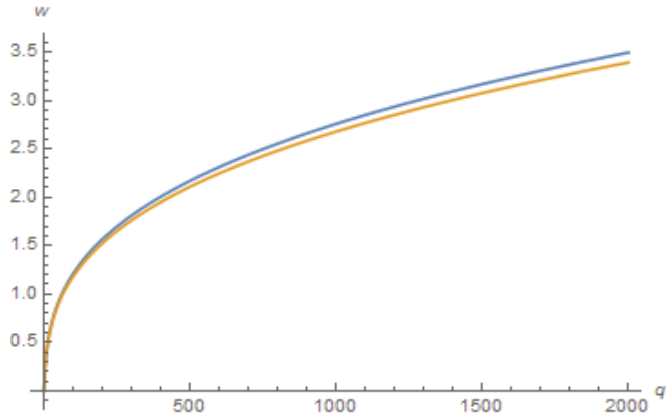

Figure 2. The dependences of the "deflection load" for otrotropic and isotropic cases. Blue line – otrotropic, yellow line -isotropic, green line- $\delta = a$, redline- $a = 0.8\delta$

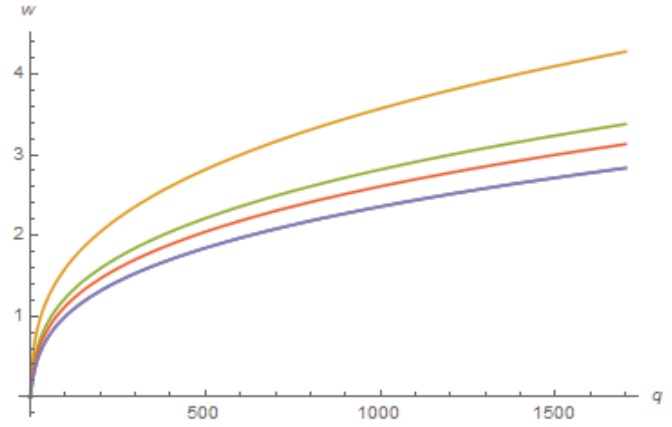

Figure 3. Figure 2. Comparison of a solid panel with a grid, depending on the distance between the edges of the lattice. Blue line –solid panel, yellow line - $a = 2\delta$, green line- $\delta = a$, red line - $a = 0.8\delta$

Taking into account the orthotropic properties of the material leads to an increase in deflections, that is, to a decrease in the bending stiffness of the panel. The greater the difference between the values of the simplicitymodulus, than more noticeable will be the described effect.When obtaining numerical results, an important issue is their reliability. Mathematical models of vibrations of smooth shells were repeatedly compared with the results of other authors and numerical experimenters. It is shown that, as the distance between the edges of the family of the rod core decreases, the deflections of the grid approach the deflections of the continuous (Figure 2). Under these experimental conditions, their

full agreement was achieved with the following values of the geometric parameters of the grid $h = \delta = 0.6a$.

In Figure 3 shows the load-deflection graphs for various values of the curvature parameter ($k_y = \{0;16;24\}$) of the mesh ($a = 0.002$) micropolar ($l = 0.3$) panel. In the case of plate ($k_y = 0$), the graphs are in qualitative agreement with those for smooth plates.In the case of continuous shellswhen $k_y > 12$, an increase in load leads to the phenomenon of "cotton". In the case of a mesh micropolar panel, the phenomenon of "cotton" was not detected.

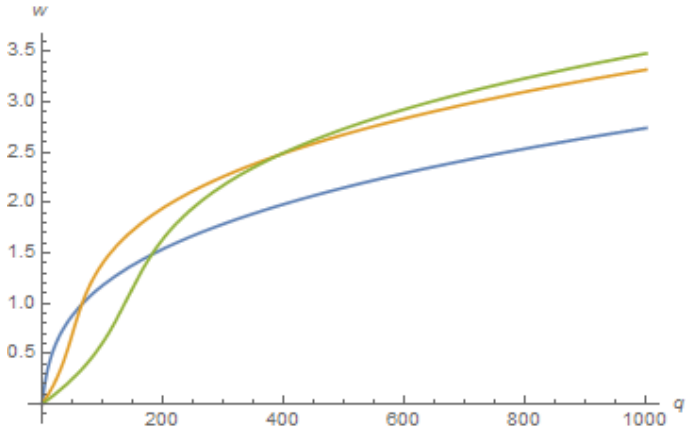

Figure 4. Dependence of the "deflection-load"graphs on the panel curvature parameter.Blue line - $k_y = 0$, yellow line - $k_y = 16$, green line- $k_y = 24$.

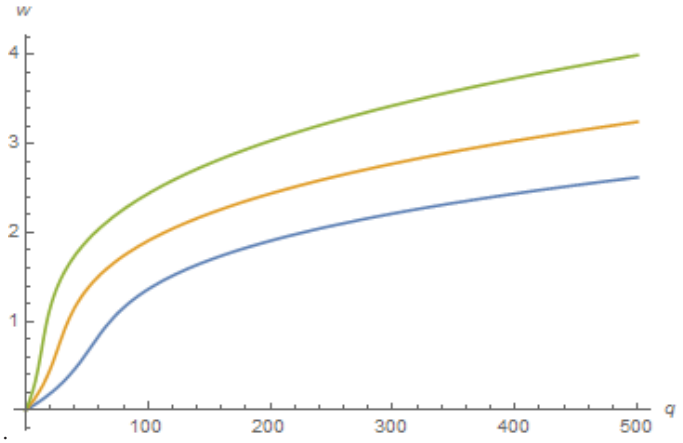

Figure 5. Dependence of the "deflection load" graphs on the distance between ribs. Blue line - $a = \delta = 0.002$, yellow line - $a = 0.004$, green line- $a = 0.008$.

In Figure 4 shows dependence of the graphs $w(q)$ for the micropolar panel with the curvature parameter $k_y = 16$ and the additional length parameter value $l = 0.3$ on the distance between ribs $a = \{0.002; 0.004; 0.008\}$. The figure shows that an increase in the distance between the ribs leads to a decrease in the bending stiffness of the panel.

3. Conclusions

On the basis of Pshenichny's continuum model and Timoshenko's hypotheses, the mathematical model of vibrations of flexible orthotropic micropolar cylindrical mesh panels is constructed.The influence of the additional length's parameter l, and mesh's geometry on the plate's behavior has been studied. The panel consists oftwo families of mutually orthogonal edges. It was revealed that, in contrast to smooth cylindrical panels of large curvature, the phenomenon of "cotton" is absent in mesh micropolar panels. Taking into account the theory of the microfield leads to an increase in the rigidity of the panel. Increasing the distance between the edges of the lattice leads to a decrease in the bending stiffness of the panel.

Acknowledgments

The work was supported by the RFBR, № 18-01-00351a, №18-41-700001 r_a.

References

[1] Pshenichnov G. I. Teoriya tonkikh uprugikh setchatykh obolochek i plastinok [Theory of thin elastic mesh shells and plates]. Moscow, Nauka, 1982. 352 p

[2] Burmistrov E.F. Simmetrichnaya deformaciya konstruktivno ortotropnyh obolochek. Izd-voSarat. Un-ta, 1962, 108s.

[3] V.P.Shevchenko Koncentraciya napryazhenij / Pod red. A. N. Guzya, A. S. Kosmodamianskogo, – K.: A.S.K., 1998. – 387 s. (Mekhanika kompozitov: V 12 t. T. 7.)

[4] Krys'ko V.A. Nelinejnaya statika i dinamika neodnorodnyh obolochek. Izd-voSarat. Un-ta, 1976, s. 216

[5]Neff P. A geometrically exact planar Cosserat shell-model with microstructure:existence of minimizers for zero Cosserat couple modulus.*Math. Models Methods Appl. Sci.*, 2007, Vol. 17, Is. 3, P. 363–392.

[6]Birsan M. On Saint-Venant's principle in the theory of Cosseratelastic shells. *Int. J. Eng. Sci.,* 2007, Vol. 45, Is. 2–8, P. 187–198.

[7] Sarkisjan S.O. Micropolar theory of thin rods, plates and shells.*Proceed*-ings National Academy of Sciences of Armenia. Mechanics – Izvestiya N N*rmenii. Mekhanika*, 2005, Vol. 58, No. 2, P. 84–95.

[8] Krylova E Yu, Papkova I V, Sinichkina A O, Yakovleva T B, Krysko-yang V A Mathematical model of flexible dimension-dependent mesh plates IOP Conf. Series: Journal of Physics: Conf. Series 1210 (2019) 012073 doi:10.1088/1742-6596/1210/1/012073

[9] Safarpour H., Mohammadi K. and Ghadiri M. Temperature-dependent vibration analysis of a FG viscoelastic cylindrical microshell under various thermal distribution via modified length scale parameter: a numerical solution Journal of the Mechanical Behavior of Materials 2017, Volume 26, Issue 1-2, Pages 9–24

[10] Sahmani S., Ansari R., Gholami, R., Darvizeh A. Dynamic stability analysis of functionally graded higher-order shear deformable microshells based on the modified couple stress elasticity theory Composites Part B Engineering 51 (2013) 44–53

[11] Varygina M. Numerical modeling of micropolar cylindrical shells on supercomputers with GPUs AIP Conference Proceedings 1895, 080005 (2017)

[12] Xinping Zhou Lin Wang Vibration and stability of micro-scale cylindrical shells conveying fluid based on modified couple stress theory Micro & Nano Letters 2012 Volume: 7 , Issue: 7 , p 679 – 684

[13] Sarkisjan S.O., Farmanyan A.Z. Mathenatical model of micropolar anisotropic (orthotropic) elastic thin shells PNRPU Mechanics Bulletin 2011. № 3. P. 128-145.

[14] F. Yang, A. C. M. Chong, D. C. C. Lam, and P. Tong, “Couple stress based strain gradient theory for elasticity”, Int. J. Solids Struct. 39 (2002), 2731–2743.

[15] Krylova E. Yu., Papkova I. V., Yakovleva T. V., Krysko V. A. Theory of Vibrations of Carbon Nanotubes Like Flexible Micropolar Mesh Cylindrical Shells Taking into Account Shift. Izv. Saratov Univ. (N. S.), Ser. Math. Mech. Inform., 2019, vol. 19, iss. 3, pp. 305–316 (in Russian). DOI: https://doi.org/10.18500/1816-9791-2019-19-3-305-316

Jan Awrejcewicz, Professor: Lodz University of Technology, Faculty of Mechanical Engineering, Department of Automation, Biomechanics and Mechatronics, 1/15 Stefanowskego Str., 90-924 Lodz, Poland (jan.awrejcewicz@p.lodz.pl);

Ekaterina Yu. Krylova Associate Professor: Department of Mathematics and Modeling, Saratov State Technical University, Politehnicheskaya 77, 410054 Saratov, Russian Federation (kat.krylova@bk.ru);

Irina V. Papkova Associate Professor: Department of Mathematics and Modeling, Saratov State Technical University, Politehnicheskaya 77, 410054 Saratov, Russian Federation (ikravzova@mail.ru);

Vadim A. Krysko, Professor: Department of Mathematics and Modeling, Saratov State Technical University, Politehnicheskaya 77, 410054 Saratov, Russian Federation (tak@san.ru).